Virology 483 (2015) 312–317

Contents lists available at ScienceDirect

Virology

journal homepage: www.elsevier.com/locate/yviro

Brief Communication

Infectious Bursal Disease Virus non-structural protein VP5 is not a transmembrane protein

Juan Manuel Carballeda [a,b], Guillermo Maroniche [b,c], María Soledad Lucero [a,b], Matías Richetta [a], Evangelina Gómez [a,b], Silvina Chimeno Zoth [a,b], Analía Berinstein [a,b,*]

[a] Instituto de Biotecnología, CICVyA, INTA, Castelar, Cc 25, B1712WAA, Buenos Aires, Argentina
[b] Consejo Nacional de Investigaciones Científicas y Técnicas (CONICET), Rivadavia 1917, C1033AAJ Ciudad de Buenos Aires, Argentina
[c] Facultad de Ciencias Agrarias, Universidad Nacional de Mar del Plata, Balcarce, Buenos Aires, Argentina

ARTICLE INFO

Article history:
Received 8 January 2015
Returned to author for revisions
28 January 2015
Accepted 1 May 2015
Available online 3 June 2015

Keywords:
Infectious Bursal Disease Virus
VP5
Protein localization
Membrane topology

ABSTRACT

Infectious Bursal Disease Virus (IBDV) causes a highly relevant poultry disease that affects young chickens causing, among other effects, immunosuppression. IBDV is a bi-segmented double stranded RNA virus. The smaller ORF of larger RNA segment encodes VP5, a 17-kDa non-structural protein. Although it is an important protein for viral replication cycle, the definition of its specific role and subcellular localization remains unclear.

In the present work we demonstrate, using imaging techniques, that VP5 is not a type II transmembrane protein but an intracellular membrane-associated protein. This finding might provide evidences of VP5 interaction with cellular proteins and its functions.

Introduction

Infectious Bursal Disease Virus (IBDV), a member of the *Birnaviridae* Family, genus *Avibirnavirus*, is an endemic agent in most poultry producing areas worldwide. IBDV causes an acute, highly contagious, immunosuppressive disease in chickens (Dobos et al., 1979).

IBDV is a bi-segmented double stranded RNA virus. Its genome is enclosed within a non-enveloped icosahedral capsid. The short segment of the genome (B) encodes the viral RNA polymerase (VP1). The large segment (A) contains two partially overlapping open reading frames (ORFs). The larger ORF encodes a precursor polyprotein that can be cleaved by the protease VP4 to form VP2 and VP3 (Azad et al., 1985; Hudson et al., 1986). These two structural proteins are found in the viral capsid (Dobos et al., 1979). The smaller ORF encodes VP5, a 17-kDa non-structural protein which is highly basic, cysteine-rich and vastly conserved among serotype I isolates of IBDV strains. This protein is not present in the virion but can be detected in IBDV-infected cells. Many authors have studied VP5; nevertheless, the definition of its role remains controversial. Liu and Vakharia (2006) showed that VP5 inhibits apoptosis at early stages of viral infection. Later, Wei et al. (2011) determined that the inhibition of apoptosis is given by the interaction of VP5 with PI3K and the subsequent activation of the effector Akt signaling pathway. On the other hand, Li et al. (2012) demonstrated that VP5 acts as the main viral apoptosis inducer interacting with mitochondrial ionic channels, and Wu et al. (2009) observed that the lack of VP5 expression affects viral release from infected cells but does not prevent intracellular virus production. In another study, Lombardo et al. showed that VP5 induces cell lysis. They also studied VP5 subcellular localization utilizing three different expression systems and they detected the protein associated with the Golgi system and the plasma membrane. Employing two *in silico* topology prediction programs the authors proposed that VP5 is a type II transmembrane protein with the N-terminal tail in the intracellular space and the C-terminal region exposed to the extracellular space (Lombardo et al., 2000).

In order to evaluate VP5 topology within the membrane, we utilized the fluorescence Protease Protection Assay (FPP) method developed by Lorenz et al. (2006).

In the present work we demonstrate that VP5 is not a type II transmembrane protein but an intracellular membrane-associated

* Corresponding autor at: Instituto de Biotecnología, CICVyA, INTA, Castelar, Cc25, B1712WAA, Buenos Aires, Argentina. Tel.: +54 11 4621 1278.
E-mail address: berinstein.analia@inta.gob.ar (A. Berinstein).

http://dx.doi.org/10.1016/j.virol.2015.05.003
0042-6822/

protein. Further analyses are necessary to determine the proteins to which VP5 is associated within the plasma membrane of the host cells and its significance to the virus replication cycle.

Materials and methods

Cells and plasmids

Quail muscle clone 7 (QM-7) cells (ATCC® CRL-1962™) were used for all the experiments. QM-7 cells are susceptible to IBDV infection (Irigoyen et al., 2009; Delgui et al., 2013).

To obtain VP5 gene, QM-7 cells were infected with D-78 IBDV strain. After 48 h, RNA was extracted using a TRIZOL reagent (Invitrogen™). Reverse transcription was carried out using a SuperScript III first strain kit (Invitrogen™) with specific VP5 reverse primer (AAGCTTCTCAGGCTTCCTTGGAAG). The obtained cDNA was used as template for PCR to amplify VP5 complete gene adding forward primer (GAATTCAATGGTTAGTAGAGATCAGAC). The amplified product was inserted into the pTOPO®–TA vector (Life Technologies) (pTOPO-VP5). Then, VP5 was excised and inserted into pcDNA 3 (Invitrogen™) vector using HindIII and XbaI restriction enzymes (pcDNA-VP5). CFP was obtained from vector pECFP (PT3258-5, Clontech) using XbaI, restriction enzyme and cloned into pcDNA-VP5 to obtain pVP5-CFP. YFP, without its stop codon, was obtained from pTgYFPH (Maroniche et al., 2011). YFP was excised with HindIII digestion and cloned into pcDNA-VP5 to obtain pYFP-VP5. The right orientation of all vectors was confirmed by sequencing. All restriction enzymes were purchased from New England Biolabs and digestion reactions were set up according to manufacturer's guidelines.

Also, mCherry gene was excised from pRB-mCherry Vector (R. Baltanas, unpubl. data) and inserted into pcDNA3 (pmCherry).

Plasmid pGP64-mCherry was kindly provided by Dr. Andrea Peralta (Instituto de Biotecnología, INTA, Castelar, Argentina) (Peralta et al., 2013).

Plasmid pYFP-PrP was kindly given by Dr. Holger Lorenz (University of Heidelberg, Germany). PrP is a prionic protein that is localized in plasma membrane and exposes its N-terminal extreme to the extracellular space (Lorenz et al., 2006).

All vector plasmids were also sequenced to confirm the correctness of cloning process (Sequence and genotypifing service, INTA, Castelar, Argentina).

Transfection procedure

Cells were grown, transfected, and observed on 8-well chamber slides (Nunc® Lab-Tek® II chambered coverglass). QM-7 cells were transfected with 125 ng of plasmid using lipofectamine (Gibco), following the instructions of the manufacturer. At 24 h post-transfection cells were observed using a Leica TCS-SP5 spectral laser confocal microscope (Leica Microsystems GmbH, Wetzlar, Germany).

Fluorescence microscopy and imagining

CellTracker™ CM-DiI (Life TechnologiesTM) (Texas Red membrane marker) was used to stain cell membranes. Briefly, QM-7 cells were washed with PBS. CM-DIL-Texas Red was rapidly added onto the medium (final concentration 50 μg/ml) and incubated at room temperature for 5 min with occasional agitation. Reaction was stopped by the addition of 1 ml of cold fetal calf serum (FCS) and cells were washed three times in complete culture medium at room temperature before confocal microscopic observation. We used a Leica TCS SP5 microscope and all images were analyzed using the Leica Application Suite X software. Laser confocal scanning microscopy was performed utilizing a 40X oil objective (HCX PL APO CS 40.0 × 1.25 OIL UV). The 514 nm and 458 nm lines of the Argon laser were used for YFP and CFP excitation. The 543 nm line from the HeNe laser was employed for mCherry or Texas Red excitation. Scanning was performed in sequential mode when using two fluorophores simultaneously to eliminate signal bleed-through, and fluorescence emission was detected with the following channel settings: 498–540 nm for CFP, 525–600 nm for YFP and 610–670 nm for mCherry or Texas Red. The microscope power settings, detectors gain and scanning speed were adjusted to optimize contrast and resolution for each individual image.

Fluorescence Protease Protection Assay (FPP)

QM-7 cells seeded in 8 well-plates (Nunc® Lab-Tek® II chambered coverglass) were transfected with pYFP-VP5, pVP5-CFP or pYFP-PrP plasmid and pmCherry and FPP assay was performed as previously described (Lorenz et al., 2006). Briefly, Twenty four hours post-transfection, the growth medium was replaced with PBS and the cells were treated with either 50 μM digitonin (Sigma-Aldrich) or 5 μM/ml proteinase K (Invitrogen™) during real-time confocal laser scanning microscopy. pYFP-PrP plasmid was kindly gifted by Dr. Holger Lorenz (Goethe-Universität, Frankfurt, Germany) and it was used as a control for the FPP assay.

Western blot assays

Protein association with membranes was analyzed by Western blot assay. Briefly, QM-7 cells were seeded in 6-wells plates to reach 70% of confluence. Then, cells were transfected with 5 μg of pYFP-VP5, pYFP-PrP or pYFP. At 24 h post-transfection, cells were disrupted by passing through 27 G syringe. The membrane fraction (M) was separated from the lysate (L) by ultracentrifugation (100,000 g, 30 min). Fractions obtained were resolved by SDS-PAGE, transferred to a nitrocellulose membrane and detected using rabbit anti-GFP and anti rabbit phosphatase alkaline conjugated antibodies (Sigma®) and NBT/BCIP (Promega®) reaction.

Results

VP5 localizes in the plasma membrane of QM-7 cells

To determine the subcellular localization of VP5 in avian cells, QM-7 cells were transfected with the expression vectors pYFP-VP5 and pVP5-CFP. We observed that both VP5 fusion proteins localized in the plasma membrane (Fig. 1). Cells conserved their form and size and the fluorescence was constant all around the plasma membrane, regardless the position of the fluorescent protein. To further confirm the membrane localization of VP5 in our system, cells were co-transfected with the plasmid pGP64-mCherry, which contains the baculoviral envelope protein GP64 which localizes in the plasma membrane of insect cells (Peralta et al., 2013) fused to mCherry, and both VP5 CFP or YFP fusion. As it can be observed in Fig. 1A, VP5 fusions and GP64-mCherry co-localized in the plasma membrane of QM-7 cells. Also, CM-DIL-Texas Red membrane marker was used to stain pVP5-CFP transfected cells. We observed a co-localization of the fluorescent marker with VP5 fusion (Fig. 1B). In summary, we corroborated by two different assays the cell membrane localization of VP5 in QM-7 cells.

To analyze whether VP5 is retained in the cell membrane or is localized close to it, we co-transfected pYFP-VP5 and pRBmCherry [a red fluorescent protein under the regulation of the CMV promoter that localizes in cytoplasm and nucleus (Maroniche et al., 2012)] plasmids into QM-7 cells, and treated the cells with digitonin for membrane permeabilization. *In vivo* imaging of the

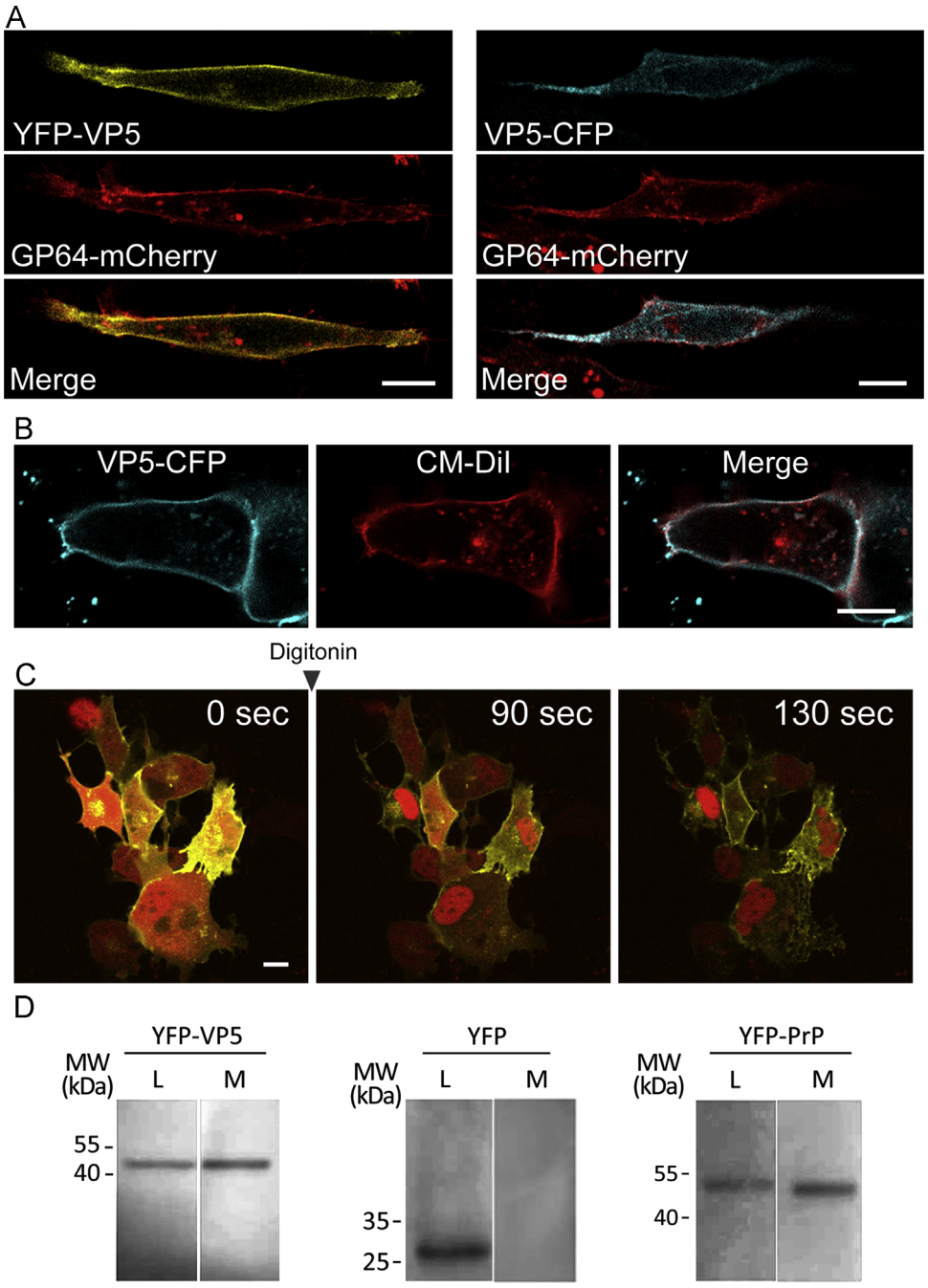

Fig. 1. VP5 subcellular localization. (A) Cells were co-transfected with pYFP-VP5, or pVP5-CFP, and pGP64 - mCherry, a plasma membrane protein marker. In both cases, cells were observed at 24 h post-transfection by confocal microscopy. (B) QM-7 cells were transfected with the pVP5-CFP construction. 24 h post-transfection, cells were stained with plasma membrane specific dye CM-DIL-Texas Red. Cells were observed by confocal microscopy with adjusted parameters to each fluorescent emission. (C) QM-7 cells were co-transfected with a mCherry expressing plasmid and with pYFP-VP5. 24 h post-transfection cells were treated with 50 μM of digitonin to permeabilize plasma membrane. Cells images were registered in real time before and after digitonin addition. The figure shows image captures at 3 and 5 s after digitonin addition. Scale bar corresponds to 10 μm. (D) QM-7 cells were transfected with pYFP-VP5, pYFP-PrP or pYFP. At 24 h post-transfection, cells were disrupted. The membrane fraction (M) was separated from the lysate (L) by ultracentrifugation. Fractions obtained were resolved by SDS-PAGE and detected using rabbit anti-GFP and alkaline conjugated antibodies.

treated cells showed the persistence of YFP fluorescence in the membrane and the dispersion of cytoplasmic mCherry red fluorescence, indicating that VP5 is retained in the plasma membrane of co-transfected cells (Fig. 1C). Moreover, nuclear red fluorescence was retained in the nucleus indicating that digitonin mediated permeabilization was restricted only to the plasma membrane.

To further corroborate our results, we transfected QM-7 cells with pYFP-VP5, pYFP-PrP or pYFP, we disrupted the cells and separated the membrane fraction (M) by ultracentrifugation. Fractions were resolved by SDS-PAGE and visualized by immunoblotting using anti-GFP antibodies (Fig. 1D). As can be observed, both PrP and VP5 proteins are detected associated to membranes; on the other hand, YPF is only detected in the lysate. In this way, we are confirming VP5 membrane localization.

VP5 is not a transmembrane protein

To further explore VP5 association to the plasma membrane, we performed the FPP assay. This method is based on the accessibility of proteases to a fluorescent domain fused to a

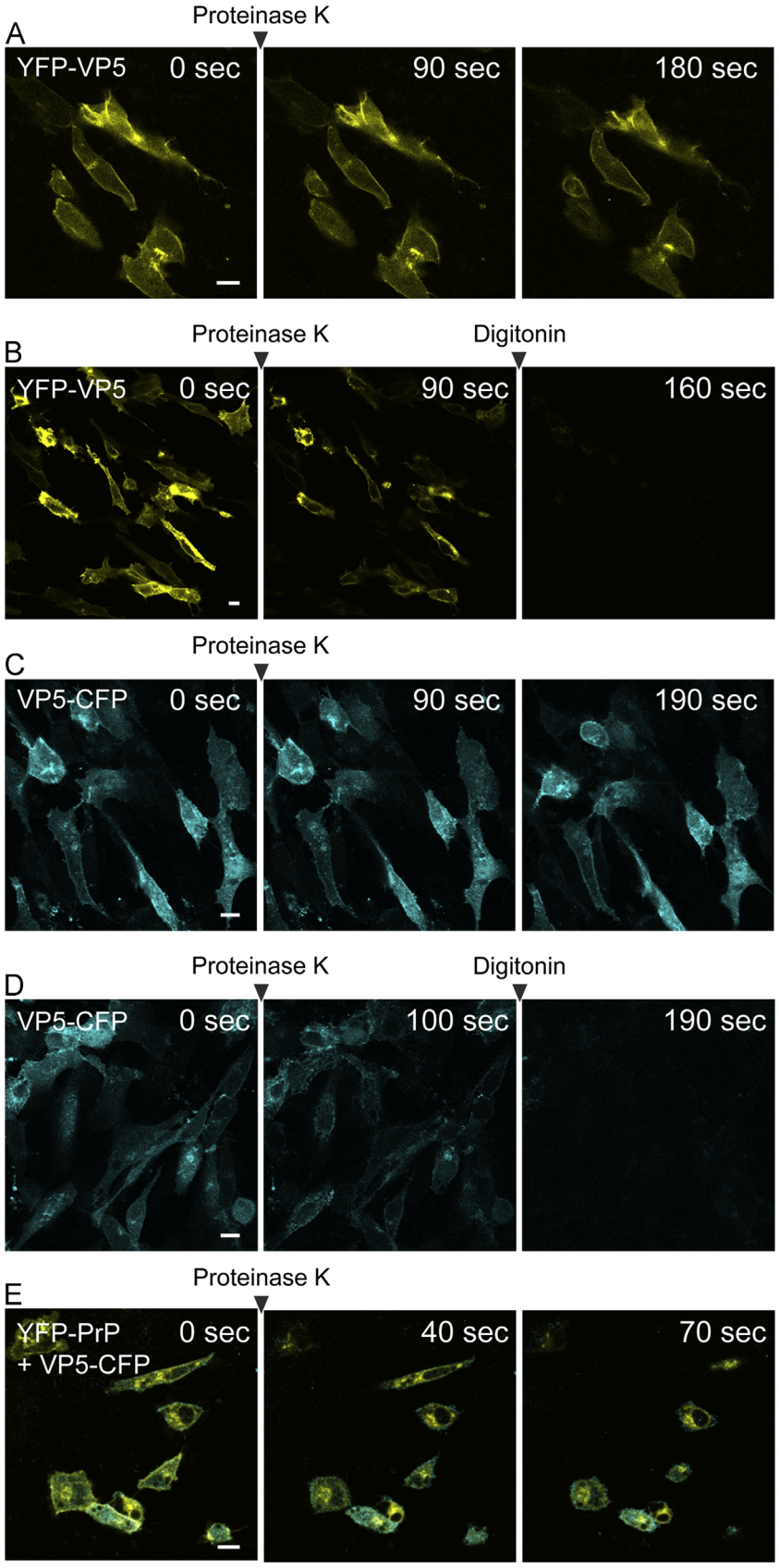

Fig. 2. Fluorescent Protease Protection Assay. (A–D) QM-7 cells were transfected with N and C-terminal VP5 fusion vectors and observed in a confocal microscope at 24 h post-transfection. *In vivo* imaging was performed in real time during the addition of digitonin and/or Proteinase K in two steps. Image captures were taken every two-second intervals. (E) The same experiment was performed with QM-7 YFP N-terminal fusion to PrP (a gene that expresses a known transmembrane protein that exposes the N-terminal domain to the extracellular space) and pVP5-CFP co-transfection. Scale bar corresponds to 10 μm.

Table 1
In silico transmembrane predictions for VP5. Public available transmembrane domains predictors were run with VP5 amino acid sequence. (GI:251765133 (Soroa Strain) and GI: 1811138 (LZD strain)).

Predictor name	Result	Transmembrane region (1–145)	References
TMpred	Transmembrane domain. N-terminus inside the cell.	69–88	(Hofmann and Stoffel, 1993)
Octopus	No transmembrane domain.		(Viklund and Elofsson, 2008)
DAS	Transmembrane domain.	72–78	(Cserzö et al., 1997)
Protter	No transmembrane domain		(Omasits et al., 2014)
Split	Transmembrane domain	68–80	(Juretić et al., 2002)
TopPred	Transmembrane domain	64–73	(Claros and von Heijne, 1994)
PRODIV-TMHMM	No transmembrane domain		(Viklund and Elofsson, 2004)
SOSUI	Soluble protein		(Mitaku et al., 1998)
HMMTOP	No transmembrane domain		(Tusnády and Simon, 2001)
TOPCONS	No transmembrane domain		(Bernsel et al., 2009)

protein of interest and expressed in living cells. If the protein under study exposes the fluorescent domain to the extracellular space, the protease will proteolise it, turning off the fluorescence (Lorenz et al., 2006).

When the assay was performed on pYFP-VP5 transfected cells, the addition of proteinase K did not affect the fluorescence observed, meaning that the amino-terminal extreme of VP5 is not exposed to the extracellular space (Fig. 2A). As expected, when digitonin was also added, the proteinase K had access to the interior of the cells and digested the fluorophore (Fig. 2B). Interestingly, the same effect was seen when the assay was performed on pVP5-CFP transfected cells (Fig. 2C and D), indicating that the carboxy-terminal extreme of VP5 was not exposed to the extracellular space either. On the other hand, when the assay was performed on pYFP-PrP and pVP5-CFP cotransfected cells the results obtained were as expected for a transmembrane protein exposing its N-terminal extreme to the extracellular space for PrP, while CFP from VP5-CFP fusion still remained in plasma membrane (Fig. 2E). We tested the ability of the proteinase K to degrade CFP repeating the experiment with QM-7 cells transfected with pCFP-PrP (data not shown). In this case, again, the addition of proteinase K digested the fluorophore indicating that both YFP and CFP can be proteolized by the protease used. Similar results were obtained when the assays were performed using chicken embryo fibroblast (data not shown).

These results showed that neither the VP5 carboxy-terminal nor its amino-terminal tail are exposed to the extracellular space.

In addition, *in silico* analysis performed on different current available bioinformatics tools are not consistent in VP5 localization (Table 1). Although some predictors indicate VP5 as a transmembrane protein, others do not. We also compared different VP5 available sequences with the transmembrane/topology prediction algorithms and the analyses showed that all VP5 had the same localization, regardless the aminoacid variation they could have. We indeed tested several VP5 sequences from other strains of IBDV and even when the apolar region showed sequence variations, we found no differences between them.

Discussion

Studying a protein localization at the subcellular level is of great importance because this information might lead to a better understanding of the protein function, interaction networks and cellular signaling pathways (Stadler et al., 2013). In a recent work, Delgui and coworkers studied the cellular localization of IBDV protein VP3 using HeLa and QM-7 cells. They determined the key role of all IBDV RNPs localization in early endosomal structures, forming ministacks with outer side of Golgi apparatus membrane. The authors, using a similar approach to the one used in this study, also observed the cellular localization of recombinant IBDV VP3 in QM-7 cells (Delgui et al., 2013).

In this work, we studied the *in vivo* subcellular localization of IBDV VP5 in avian cells using fluorescent proteins as fusion partners. Experiments were performed with amino and carboxy-terminal fusions due to possible interferences in the localization and function of VP5 (Palmer and Freeman, 2004). In accordance with previous works (Lombardo et al., 2000), we found that VP5 of IBDV is associated with the plasma membrane when fused to fluorescent proteins either by its carboxy-terminal or amino-terminal end (Fig. 1). As far as we know, this is the first study that provides the localization analysis of VP5 using *in vivo* imaging and avian cells.

Next, we analyzed VP5 topology using the FPP assay (Lorenz et al., 2006) on transfected avian cells and we found that the carboxy- as well as the amino-terminal region of VP5 are in contact with the cytoplasm of host cells (Fig. 2). Lombardo et al. (2000) postulated that VP5 was a type II transmembrane protein by following *in silico* prediction models that recognize VP5 as a membrane protein based on the presence of a hydrophobic domain, which is not a consensus for transmembrane proteins. Our experimental results strongly support the idea that VP5 is not a transmembrane protein but is rather associated, directly or indirectly, to the inner face of the plasma membrane. This is a novel unexpected result that opens new questions regarding protein function and IBDV replication cycle. There are no reports on transmembrane/topology predictions for VP5 from other birnaviruses. We found that all algorithms we used, predicted VP5 from IPNV as a protein without transmembrane domain (data not shown).

VP5 subcellular localization and topology provides new evidence for the protein interaction possibilities. The apoptotic or anti-apoptotic role of VP5 was discussed in previous works (Liu and Vakharia, 2006; Wei et al., 2011; Li et al., 2012). Wei et al. demonstrated that VP5 inhibits early apoptosis by interacting with the regulatory (p85) alpha subunit of PI3K which is located in the plasma membrane (Mandelker et al., 2009), and the interaction between VP5 and PI3K is critical for the apoptosis protection phenomenon. In that regard, the fact that VP5 has no extracellular domains expands the possibilities of interaction with PI3K by both its C or N-terminal domains.

Current studies are focusing on the relationship between VP5 and hosts cells factors that contributes to attach the viral protein to the internal side of the plasma membrane such us yeast double hybrids and immunoprecipitation.

Acknowledgments

The authors are grateful to Dr. Holger Lorenz and Dra. Andrea Peralta for the pYFP-PrP, pCFP-PrP and pGP64-mCherry plasmids

respectively. This work was supported by Grant PE 1131034 from INTA, Argentina. JMC and SL are recipients of CONICET fellowship. MR is recipient of ANPCyT fellowship.

References

Azad, A.A., Barrett, S.A., Fahey, K.J., 1985. The characterization and molecular cloning of the double-stranded RNA genome of an Australian strain of infectious bursal disease virus. Virology 143, 35–44.

Bernsel, A1, Viklund, H., Hennerdal, A., Elofsson, A., 2009. TOPCONS: consensus prediction of membrane protein topology. Nucleic Acids Res. 37 (Web Server issue),W465-8.

Claros, M.G., von Heijne, G., 1994. TopPred II: An improved software for membrane protein structure predictions. CABIOS 10, 685–686.

Cserzö, M., Wallin, E., Simon, I., von Heijne, G., Elofsson, A., 1997. Prediction of transmembrane alpha-helices in prokaryotic membrane proteins: the dense alignment surface method. Protein Eng. 10 (6), 673–676.

Delgui, L.R., Rodriguez, J.F., Colombo, M.I., 2013. The endosomal pathway and the Golgi complex are involved in the infectious bursal disease virus life cycle. J. Virol. 87, 8993–9007.

Dobos, P., Hill, B.J., Hallett, R., Kells, D.T., Becht, H., Teninges, D., 1979. Biophysical and biochemical characterization of five animal viruses with bisegmented double-stranded RNA genomes. J. Virol. 32, 593–605.

Hudson, P.J., McKern, N.M., Power, B.E., Azad, A.A., 1986. Genomic structure of the large RNA segment of infectious bursal disease virus. Nucleic Acids Res. 14, 5001–5012.

Hofmann, K., Stoffel, W., 1993. TMbase A database of membrane spanning proteins segments. Biol. Chem. Hoppe-Seyler 374, 166.

Irigoyen, N., Garriga, D., Navarro, A., Verdaguer, N., Rodriguez, J.F., Caston, J.R., 2009. Autoproteolytic activity derived from the infectious bursal disease virus capsid protein. J. Biol. Chem. 284, 8064–8072.

Juretić, D1, Zoranić, L., Zucić, D., 2002. Basic charge clusters and predictions of membrane protein topology. J. Chem. Inf. Comput. Sci. 42 (3), 620–632.

Li, Z., Wang, Y., Xue, Y., Li, X., Cao, H., Zheng, S.J., 2012. Critical role for voltage-dependent anion channel 2 in infectious bursal disease virus-induced apoptosis in host cells via interaction with VP5. J. Virol. 86, 1328–1338.

Liu, M., Vakharia, V.N., 2006. Nonstructural protein of infectious bursal disease virus inhibits apoptosis at the early stage of virus infection. J. Virol. 80, 3369–3377.

Lombardo, E., Maraver, A., Espinosa, I., Fernandez-Arias, A., Rodriguez, J.F., 2000. VP5, the nonstructural polypeptide of infectious bursal disease virus, accumulates within the host plasma membrane and induces cell lysis. Virology 277, 345–357.

Lorenz, H., Hailey, D.W., Lippincott-Schwartz, J., 2006. Fluorescence protease protection of GFP chimeras to reveal protein topology and subcellular localization. Nat. Methods 3, 205–210.

Mandelker, D., Gabelli, S.B., Schmidt-Kittler, O., Zhu, J., Cheong, I., Huang, C.H., Kinzler, K.W., Vogelstein, B., Amzel, L.M., 2009. A frequent kinase domain mutation that changes the interaction between PI3Kalpha and the membrane. Proc. Natl. Acad. Sci. U S A 106, 16996–17001.

Maroniche, G.A., Mongelli, V.C., Alfonso, V., Llauger, G., Taboga, O., del Vas, M., 2011. Development of a novel set of Gateway-compatible vectors for live imaging in insect cells. Insect Mol. Biol. 20, 675–685.

Maroniche, G.A., Mongelli, V.C., Llauger, G., Alfonso, V., Taboga, O., del Vas, M., 2012. *In vivo* subcellular localization of Mal de Rio Cuarto virus (MRCV) non-structural proteins in insect cells reveals their putative functions. Virology 430, 81–89.

Mitaku, S., Hirokawa, T., Ono, M., 1998. Classification of membrane proteins by types of transmembrane helices using SOSUI system. Genome Informat. 9, 367–368.

Omasits, U., Ahrens, C.H., Muller, S., Wollscheid, B., 2014. Protter: interactive protein feature visualization and integration with experimental proteomic data. Bioinformatics 30, 884–886.

Palmer, E., Freeman, T., 2004. Investigation into the use of C- and N-terminal GFP fusion proteins for subcellular localization studies using reverse transfection microarrays. Comp. Funct. Genomics 5, 342–353.

Peralta, A., Maroniche, G.A., Alfonso, V., Molinari, P., Taboga, O., 2013. VP1 protein of Foot-and-mouth disease virus (FMDV) impairs baculovirus surface display. Virus Res. 175, 87–90.

Stadler, C, Rexhepaj, E, Singan, VR, Murphy, RF, Pepperkok, R, Uhlen, M, Simpson, JC, Lundberg, E., 2013. Immunofluorescence and fluorescent-protein tagging show high correlation for protein localization in mammalian cells. Nat. Methods 10, 315–323.

Tusnády, GE., Simon, I., 2001. The HMMTOP transmembrane topology prediction server. Bioinformatics 17, 849–850.

Wei, L., Hou, L., Zhu, S., Wang, J., Zhou, J., Liu, J., 2011. Infectious bursal disease virus activates the phosphatidylinositol 3-kinase (PI3K)/Akt signaling pathway by interaction of VP5 protein with the p85alpha subunit of PI3K. Virology 417, 211–220.

Wu, Y., Hong, L., Ye, J., Huang, Z., Zhou, J., 2009. The VP5 protein of infectious bursal disease virus promotes virion release from infected cells and is not involved in cell death. Arch. Virol. 154, 1873–1882.

Viklund, H., Elofsson, A., 2004. Best alpha-helical transmembrane protein topology predictions are achieved using hidden Markov models and evolutionary information. Protein Sci. 13 (7), 1908–1917.

Viklund, H., Elofsson, A., 2008. OCTOPUS: improving topology prediction by two-track ANN-based preference scores and an extended topological grammar. Bioinformatics 24, 1662–1668.